

## Short Communication

Local chemo-mechanical insights into the efficacy of ZDDP additives from *in situ* single asperity growth and mechanical testingXuying Liu<sup>a</sup>, Ching-Yen Tang<sup>a</sup>, Rui Hao<sup>a</sup>, Kathleen Walsh<sup>b</sup>, Chunliang Zhou<sup>c</sup>, Shen J. Dillon<sup>a,b,\*</sup><sup>a</sup> Department of Materials Science and Engineering, University of Illinois Urbana-Champaign, Urbana, IL, USA<sup>b</sup> Materials Research Laboratory, University of Illinois Urbana-Champaign, Urbana, IL, USA<sup>c</sup> School of Power and Nuclear Energy Engineering, Harbin Engineering University, Harbin, 150001 Heilongjiang, PR China

## ARTICLE INFO

## Keywords:

ZDDP  
Mechanical properties  
Chemistry  
TEM

## ABSTRACT

This work combines nanoscale tribological wear methods, used to prepare zinc dialkyldithiophosphate (ZDDP) tribofilms under conditions of controlled loading, with site specific nanopillar compression testing to derive a relationship between the ZDDP growth conditions and resultant mechanical properties. The key finding is that ZDDP films grown at higher loads exhibit lower yield strengths, which correlate with differences in tribofilm chemistry. We hypothesize that the load sensitivity of tribofilm properties may underlie the efficacy of ZDDP in suppressing wear by functioning as a hard coating at low loads while exhibiting enhanced lubricity at high loads.

## 1. Introduction

Engineering optimized lubricant additives underlies the efficient function of engines and mechanical systems. Antiwear additives improve system lifetime and have become increasingly important in engines functioning in ever more extreme environments [1]. The most successful and prolific antiwear additive, zinc dialkyldithiophosphate (ZDDP), has been an important lubricant component since the 1940's [2–4]. The removal of lead from automotive fuels placed ZDDP amongst the most important antiwear additives for automotive applications. However, phosphorous and sulfur tend to poison metal nanoparticle catalysts present in catalytic converters [5]. This fact motivates significant efforts in the last two decades to reduce or replace ZDDP. Suitable complete replacements have evaded discovery partially owing to our limited understanding of the deformation mechanisms of ZDDP during wear and the fundamental properties underpinning its efficacy [6].

Elucidating the fundamental constitutive properties of ZDDP underlying its antiwear efficacy presents challenges due to both the chemomechanical complexity of wear and the chemical heterogeneity of ZDDP tribofilms [3,7–12]. ZDDP films typically contain glassy phosphates, zinc polyphosphates, zinc sulphides, and when grown on metallic substrates the films also contain other metal sulphides and oxides [3,13,14]. The chemical distribution in tribofilms exhibit spatial heterogeneity on the micron and nanoscale both laterally and out of plane [15–17]. This distribution may result in part from the thermo-mechanical nature of ZDDP tribofilm formation, where they can grow

via a thermally activated decomposition at elevated temperatures, stress dependent mechanically activated contact sliding at lower temperatures, or a synergistic combination of the two effects [6,12]. Tribological stress during sliding wear inherently localizes at micro-scale and nanoscale asperities, which likely induces the chemical heterogeneity observed in tribofilms. Kinetic growth models for ZDDP tribofilm formation as a function of stress and temperature were recently established based on single asperity contact growth studies using diamond coated atomic force microscope tips [6]. The growth rate was given by,

$$\Gamma = \Gamma_0 \exp\left(-\frac{\Delta U - \sigma \Delta V}{kT}\right)$$

where  $U$  is the internal activation energy,  $V$  is the activation volume,  $\sigma$  is applied stress,  $kT$  is the thermal energy. While the data could be fit well to a single activation energy ( $\Delta U \approx 0.8$  eV) and activation volume ( $\Delta V \approx 3.8 \text{ \AA}^3$ ), it remains to be determined whether the properties of the tribofilm that forms under different conditions are also nominally determined by a single descriptor. A number of nanoindentation based hardness values have been reported in the literature and range from 1 to 10 GPa with significant variations observed even within individual samples [8,16,18–25]. The discrepancies in the data suggest that the mechanical properties may in fact be sensitive to the local growth conditions and are inherently spatially heterogeneous. While efforts have been made in prior studies to correlate hardness and chemistry, the local growth conditions are not well known for bulk tribolayer formation. Indentation hardness measurements are not ideal for

\* Corresponding author at: Department of Materials Science and Engineering, University of Illinois Urbana-Champaign, Urbana, IL, USA.  
E-mail address: [sdillon@illinois.edu](mailto:sdillon@illinois.edu) (S.J. Dillon).

spatially heterogeneous materials because they sample volumes much larger than the indent size. They may also be subject to substrate induced artifacts, particularly in films of unknown local thickness. However, the prior observations motivate the two primary questions being investigated here: i) are the properties of ZDDP tribofilms sensitive to growth load and, if so, ii) what are the correlations between growth conditions, chemistry, and film properties?

The emergence of single asperity ZDDP growth techniques and site-specific nanopillar mechanical properties characterization provide an unprecedented opportunity to correlate tribofilm growth conditions and their associated properties [6,26–28]. In this effort, we induce localized tribofilm growth from 1% ZDDP polyalpha olefin solutions onto silicon wafers under contact sliding of a 2.5  $\mu\text{m}$  diameter cono-spherical diamond tip under different applied loads at 80 °C. Si serves as a model substrate to characterize the inherent properties of the ZDDP free of artifacts associated with chemical reactions with the substrate. We characterize the chemistry of the deposited tribofilms via energy dispersive spectroscopy (EDS) and auger electron spectroscopy (AES), and quantify their mechanical properties through in-situ transmission electron microscopy based nanopillar compression. The experimental approach allows us to directly correlate the relationship between single-asperity growth conditions and the resultant materials properties, providing new insights into the factors governing the performance of ZDDP tribolayers.

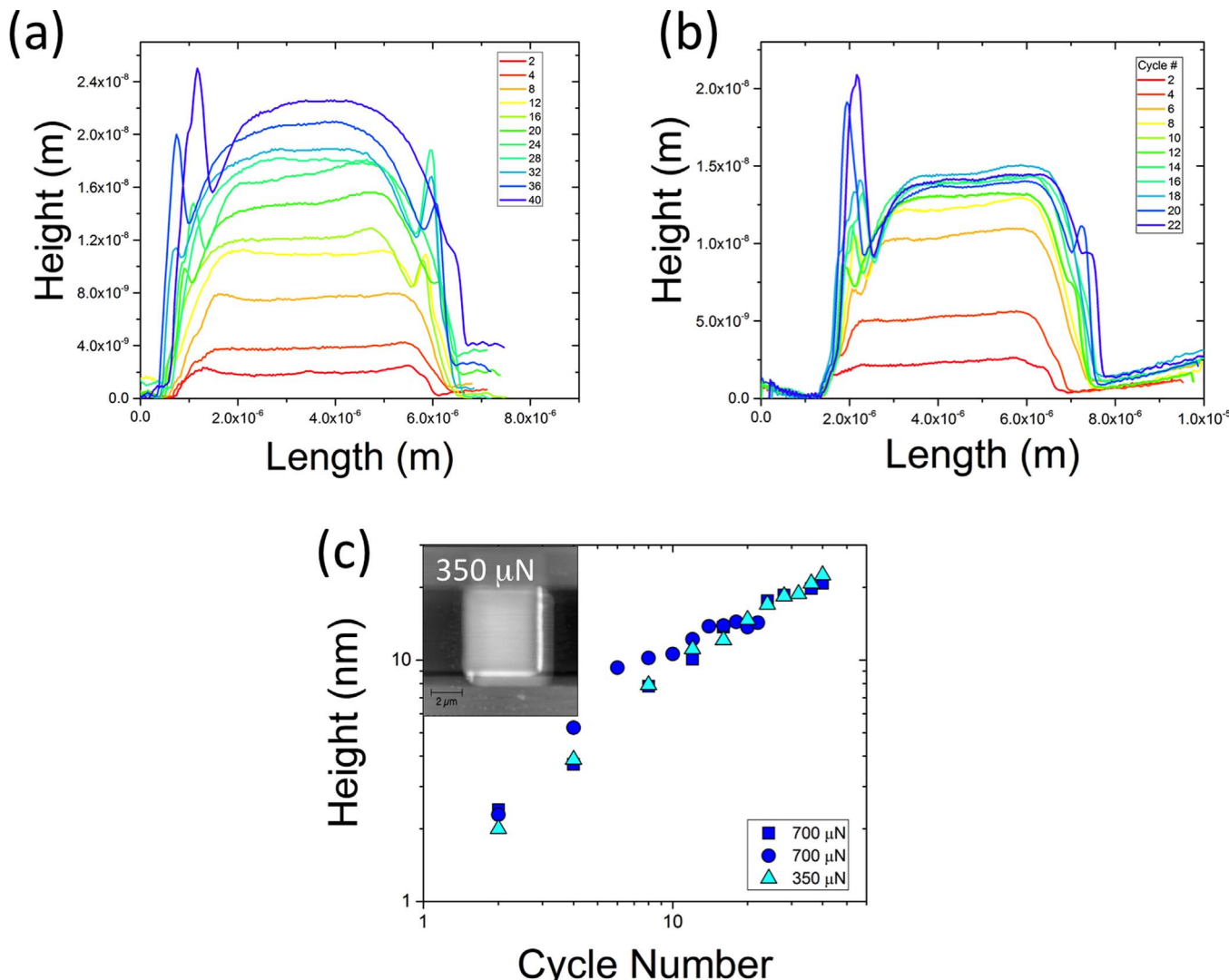
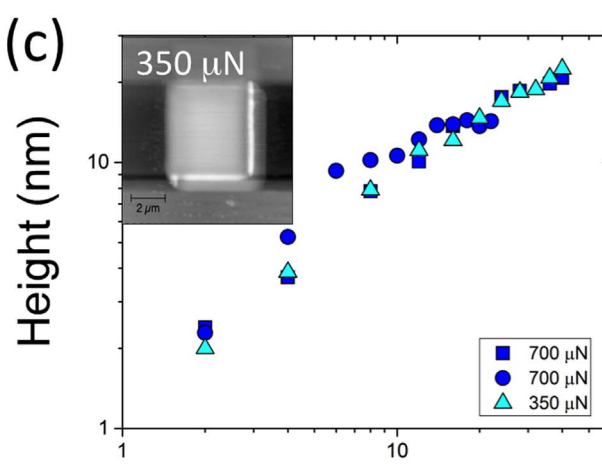
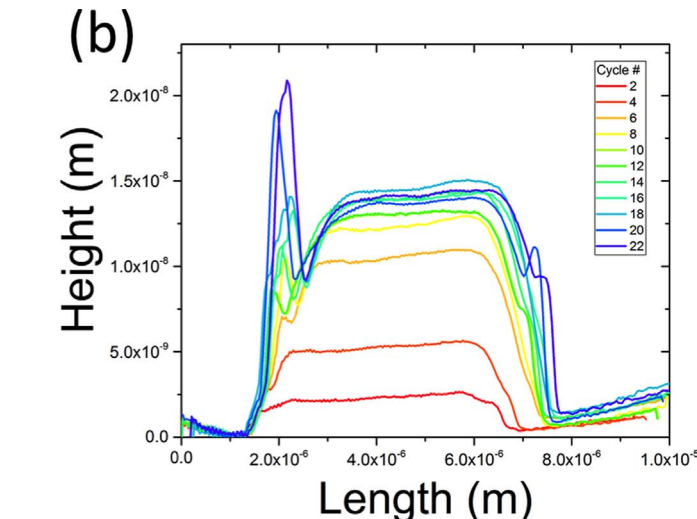


**Fig. 1.** Height profiles measured in-situ during ZDDP tribolayer growth at (a) 350  $\mu\text{N}$  and (b) 700  $\mu\text{N}$ . The height versus cycle number is plotted in (c) along with an example scan probe topographic of the film obtained in-situ.

## 2. Experimental methods

We prepared synthetic base-stock by mixing of 3.3 wt% commercial break-in oil additive (containing 30 wt% Zinc Dialkyldithiophosphate) with 96.7 wt% Dec-1-ene (homopolymer hydrogenated, 100 wt%, INEOS Oligomers, Feluy, Belgium). The base-stock was placed in an aluminum pan and contacted to a heating stage with silver paste. Pre-cleaned Si wafers were immersed in the oil and heated to 80 °C. Tribofilms were grown under a 2.5  $\mu\text{m}$  cono-spherical diamond tip (90°, VR25736, Micro Star Technologies, Huntsville, TX) in a TI-950 Tribolayer (Hysitron, Inc., Minneapolis, MN). Films were grown at a 3 Hz scan rate and different loads between 175  $\mu\text{N}$  and 700  $\mu\text{N}$  in 5  $\mu\text{m} \times 5 \mu\text{m}$  squares. Thermal films with similar thickness were grown in the same base stock at 150 °C for 13 h on Si substrates. The films were cleaned by rinsing in hexane (98.5%, Fisher Scientific, Hampton, NH) to remove remaining base-stock and dried in an Ar filled glove box. Auger electron spectroscopy was performed in a PHI 660 scanning Auger microscope. Raman spectra were obtained on a Horiba confocal Raman using a 532 nm laser source (Fig. S2).

In order to protect the films and provide a contacting plane during nanocompression, 300 nm thick Cr (99.95%, Lesker) layers were deposited on top of the films by Magnetron Sputtering (AJA International INC. N Scituate) under 3 mTorr Ar with a base pressure below 10<sup>-6</sup> Torr. Nanopillar samples were fabricated through focused



ion beam lift out (FEI Helios), mounted on wedge-shaped Si substrates, and milled to final diameter of  $\approx 300$  nm with an aspect ratio of  $\approx 2:1$ – $3:1$ . The top of each pillar was cut to provide a flat contact surface for subsequent nanocompression testing in the transmission electron microscope (TEM, JEOL 2010 LaB6 200 kV). Pillars were compressed in displacement-control mode at a rate of  $1 \text{ nm s}^{-1}$  with a  $2 \mu\text{m}$  diameter flat diamond punch (PI 95 TEM PicoIndenter, Hysitron, Inc., Minneapolis, MN). The mean values are reported from multiple measurements with error reported as one standard deviation.

### 3. Results and discussion

Fig. 1 shows the evolution of a tribofilm grown at  $350 \mu\text{N}$  imaged intermittently in-situ in the liquid. A relatively smooth and continuous deposit results from just a few cycles and grows approximately linearly with cycle number up to 40 cycles. Similar growth behavior is observed at each load. The general growth behavior is consistent with prior work by Gosvami et al., [6] although the growth rate per cycle is higher and the surface roughness is lower. Assuming maximum Hertzian contact, this material was grown at an approximate pressure of  $\approx 2 \text{ GPa}$ . Gosvami et al. reported growth rates at  $80^\circ\text{C}$ , and similar pressures, to be  $\approx 10^2 \text{ nm}^3 \text{ s}^{-1}$ . Our rates are  $\approx 10^5 \text{ nm}^3 \text{ s}^{-1}$ , however our calculated contact areas are  $\approx 10^3$  larger. Thus accounting for contact area, the results are consistent to an order of magnitude. Normalizing by area, we measure growth rates of  $1.1 \times 10^{-2} \text{ nm s}^{-1}$ , which is also similar to bulk growth rates of  $0.9 \times 10^{-2} \text{ nm s}^{-1}$  measured by Zhang and Spikes using a 19 mm ball-on-flat contact at  $100^\circ\text{C}$  and  $\approx 2.5 \text{ GPa}$  [29]. Again, the growth rates agree to an order of magnitude, which is reasonable considering the major differences in scale. Fig. 2 shows a series of adjacent tribolayers grown at different loads imaged in-situ by the scanning probe and optically. The ability to reproducibly grow tribolayers under controlled load allows us to probe the relationships between growth conditions, chemistry and properties.

Nanopillars for compression testing were prepared by sputter coating the free surface with 300 nm of Cr necessary to protect the surface and provide a flat contact for the diamond indenter after ion milling. Site-specific focused ion beam lift-out methods were used to prepare nanopillars from ZDDP tribofilms grown under controlled loads. We also prepared nanopillars from ZDDP films thermally deposited at  $150^\circ\text{C}$  for 13 h. This time and temperature produced films that on average were of comparable thickness to the tribofilms, however the thermal films exhibited significant variability in thickness. The radial surface of the Si substrate amorphizes due to ion beam milling during pillar preparation and this amorphous layer has a similar appearance in bright-field imaging as the amorphous ZDDP film in the TEM images. To confirm the chemistry of the  $\approx 30$  nm thick

tribofilm, lying between Si and Cr, energy dispersive spectroscopy mapping was employed (Fig. S1). Fig. 3 provides example time-lapse images of nanopillar compression performed using controlled displacement conditions of  $1 \text{ nm s}^{-1}$ . The lateral strain of the tribolayer was measured from the images and correlated with load measurements from the indenter (see Fig. 3). The thermally grown ZDDP tribofilm yields at  $2.43 \pm 0.19 \text{ GPa}$ , reported as experimental mean and standard deviation. The tribofilms grown at loads of  $350 \mu\text{N}$  and  $700 \mu\text{N}$  yield at  $1.16 \pm 0.08 \text{ GPa}$  and  $0.42 \pm 0.02 \text{ GPa}$ , respectively. The trend of reduced yield strength with increased processing load is rather unexpected, as most materials tend to work harden rather than work soften. However, the chemistry of ZDDP varies with growth stress in a manner that affects the underlying mechanical properties. Auger electron spectroscopy was used to map the local composition (Fig. 4) of tribofilms grown under different conditions both after cleaning the sample in hexane (Table S1) and after removing  $\approx 3$  nm of material using in situ  $\text{Ar}^+$  sputtering (Table 1). Due to the exposure of the native surface to both oil and hexane, we consider the sub-surface compositions to be more representative. The P, and S content of the tribofilms tend to decrease with increasing contact sliding load, which results in a reduce yield strength. The results support the hypothesis that local growth load experienced under asperity contact control tribofilm composition. The chemistry of this amorphous film must ultimately govern its mechanical properties. However, no fundamental basis currently exists for predicting how the properties should vary with anion composition. We note that metallic substrates on which ZDDP films are typically grown may have a catalyzing effect on the ZDDP decomposition reaction that would cause the chemistry to differ on different substrates [2,30]. However, utilizing a chemically inert substrate here demonstrates an inherent sensitivity of ZDDP tribofilm chemistry and properties to growth stress. In fact, Shimizu and Spikes found that initial tribofilm formation on Fe alloys is S rich, and subsequently becomes more Zn and P rich [31]. However, it is reasonable to expect that S will have stronger bonding interactions with Fe than the Si-O terminated substrate utilized here. This could explain why our films initially grow more Zn and P rich.

We postulate that the growth stress dependence of yield strength underlies the unique antiwear performance of ZDDP. Under low shear stress a hard tribofilm forms that can resist wear in a manner consistent with Archard's equation. At higher shear stresses, the more compliant tribofilm is more lubricious and favors sliding of asperities. The spatial variation in properties resulting from the heterogeneous stress distribution during wear also produces a tribofilm that is effectively a multiphase nanocomposite composed of hard and soft phases. The spontaneous nanocomposite formation that persists in steady-state and provides wear resistance at low loads and lubricity at

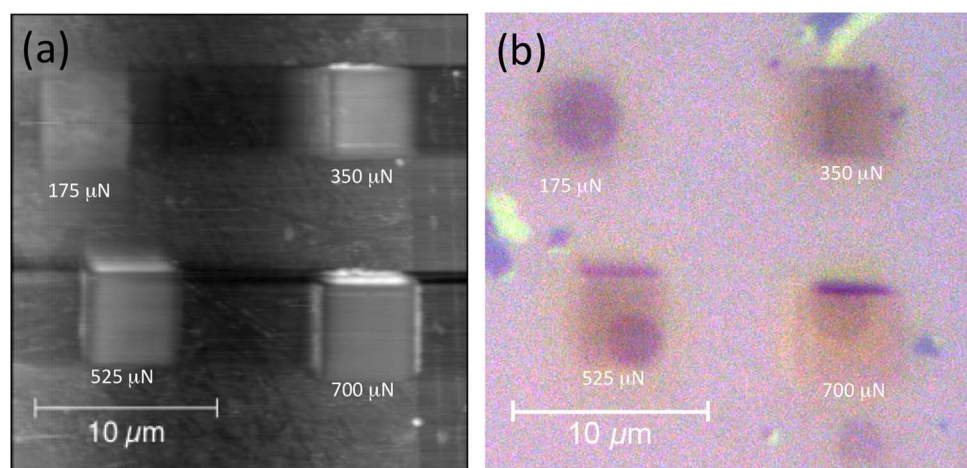
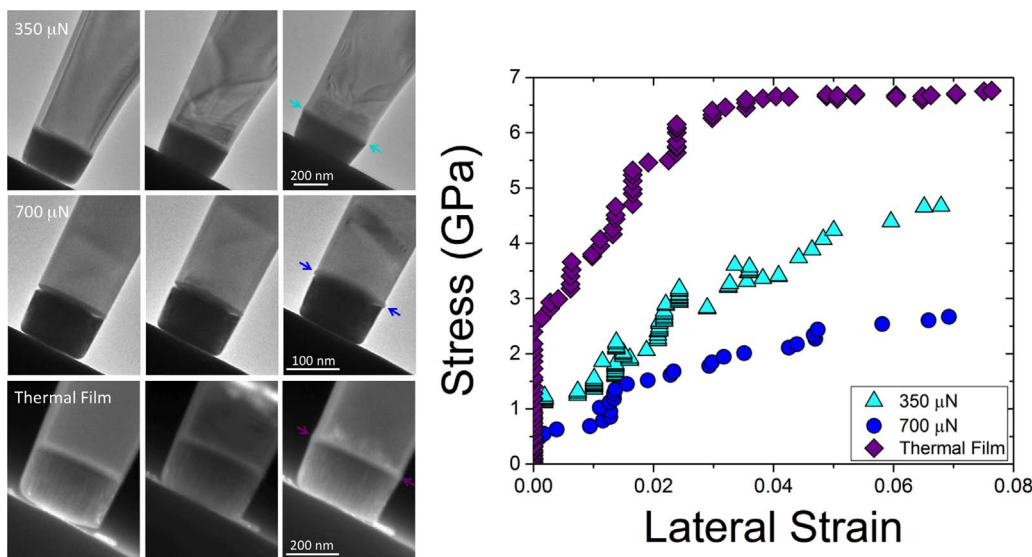
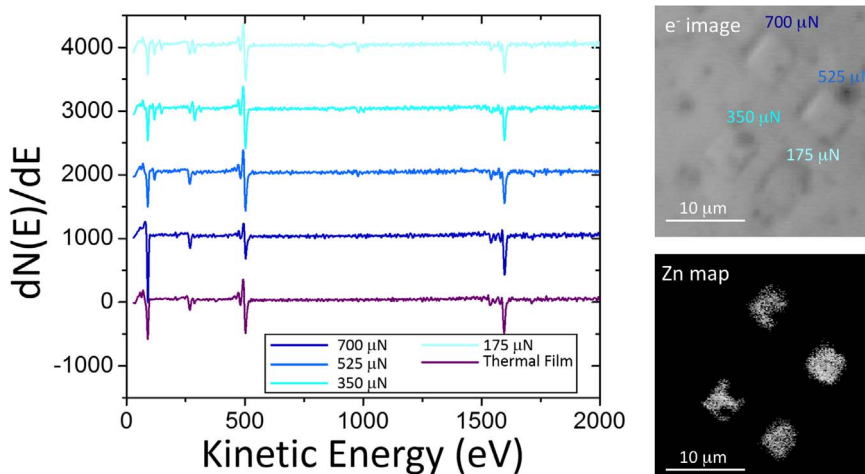


Fig. 2. Images of tribofilms obtained from nanoscale wear tests performed at  $80^\circ\text{C}$  under varying levels of load. (a) provides a topographic image obtained in-situ after growth, while (b) shows the same material imaged optically after cleaning in hexane.



**Fig. 3.** Time-lapse images obtained during in-situ nanocompression testing with examples shown for the initial loading, near the yield strength, and at high strain, along with a plot of stress versus lateral strain of the ZDDP tribofilm. The lateral strain was measured from the width of the ZDDP tribofilm in each of the images.



**Fig. 4.** Auger electron spectra for ZDDP tribofilms grown under different conditions after removing  $\approx 3$  nm via  $\text{Ar}^+$  sputtering. Note that each curve is offset by 1000 and that the data for the thermal film was rescaled to 25% of its original value such that the peak heights are comparable on the plot. The image also shows the image of the sample acquired in the AES along with a Zn map showing each of the tribofilms.

**Table 1**

Compositions of ZDDP tribofilms measured via Auger electron spectroscopy after removing  $\approx 3$  nm via  $\text{Ar}^+$  sputtering. Standard deviation values from measurements at multiple locations on the thermal film were 4%, 27%, 9%, 1%, and 6% for Zn, P, S, C, and O, respectively.

| Load (nN) | Zn  | P   | S   | C    | O    |
|-----------|-----|-----|-----|------|------|
| 700       | 3.2 | 1.4 | 0.8 | 51.9 | 42.8 |
| 525       | 3.1 | 5.8 | 0.7 | 36.3 | 54.1 |
| 350       | 3.9 | 8.2 | 3.0 | 28.3 | 56.7 |
| 175       | 5.0 | 7.3 | 2.7 | 35.0 | 49.9 |
| Thermal   | 2.1 | 0.9 | 0.4 | 40.3 | 56.3 |

high loads is anticipated to be a key feature of ZDDP's antiwear performance.

#### 4. Conclusions

This work demonstrates that the local properties of ZDDP films, grown under model conditions, correlate with differences in growth stress and consequently differences in local chemistry. We hypothesize that the dependence of chemistry and properties on local growth stress

could account for the heterogeneity in mechanical properties observed in ZDDP films. For growth on  $\text{SiO}_2$  on Si, the yield strength of the ZDDP decreased with increasing growth stress.

#### Acknowledgements

X.L. and C.-Y.T. were supported by the National Science Foundation under Grant no. 1254406. R.H. was supported by ONR-MURI under the Grant no. N00014-11-1-0678 and performed wear testing and nanomechanical testing. Experiments were performed in the F.S. Materials Research Laboratory at the University of Illinois. We would also like to acknowledge discussions with Christopher Warrens that helped inspire this experimental effort.

#### Appendix A. Supporting information

Supplementary data associated with this article can be found in the online version at doi:10.1016/j.triboint.2017.03.035.

## References

[1] Tung SC, McMillan ML. Automotive tribology overview of current advances and challenges for the future. *Tribol Int* 2004;37:517–36. <http://dx.doi.org/10.1016/j.triboint.2004.01.013>.

[2] Spikes H. The history and mechanisms of zinc dialkyldithiophosphate lubricating oil antiwear additive. *Tribol Lett* 2004;17:469–89. <http://dx.doi.org/10.1023/B:TRIL.0000044495.26882.b5>.

[3] Yin Z, Kasrai M, Fuller M, Bancroft GM, Fyfe K, Tan KH. Application of soft x-ray absorption spectroscopy in chemical characterization of antiwear films generated by ZDDP. Part I: the effect of physical parameters. *Wear* 1997;202:172–91. [http://dx.doi.org/10.1016/S0043-1648\(96\)07272-9](http://dx.doi.org/10.1016/S0043-1648(96)07272-9).

[4] Nicholls MA, Do T, Norton PR, Kasrai M, Bancroft GM. Review of the lubrication of metallic surfaces by zinc dialkyldithiophosphates. *Tribol Int* 2004;38:15–39. <http://dx.doi.org/10.1016/j.triboint.2004.05.009>.

[5] Bartholomew CH, Agrawal PK, Katzer JR. Sulfur poisoning of metals. *Adv Catal* 1982;31:135–242.

[6] Gosvami NN, Bares JA, Mangolini F, Konicek AR, Yablon DG, Carpick RW. Mechanisms of antiwear tribofilms growth revealed *in situ* by single-asperity sliding contacts. *Science* 2015;348:102–6. <http://dx.doi.org/10.1126/science.1258788>.

[7] Fuller M, Yin Z, Kasrai M, Bancroft GM, Yamaguchi ES, Ryason PR, Willermet PA, Tan KH. Chemical characterization of tribocochemical and thermal films generated from neutral and basic ZDDPs using x-ray absorption spectroscopy. *Tribol Int* 1997;30:305–15. [http://dx.doi.org/10.1016/S0301-679X\(96\)00059-X](http://dx.doi.org/10.1016/S0301-679X(96)00059-X).

[8] Nicholls MA, Do T, Norton PR, Bancroft GM, Kasrai M, Capehart TW, Cheng Y-T, Perry T. Chemical and mechanical properties of ZDDP antiwear films on steel and thermal spray coatings studied by XANES spectroscopy and nanoindentation techniques. *Tribol Lett* 2003;15:241–8.

[9] Haque T, Morina A, Neville A, Kapadia R, Arrowsmith S. Non-ferrous coating/lubricant interactions in tribological contacts: assessment of tribofilms. *Tribol Int* 2007;40:1603–12. <http://dx.doi.org/10.1016/j.triboint.2007.01.023>.

[10] Wan Y, Cao L, Xue Q. Friction and wear characteristics of ZDDP in the sliding of steel against aluminum alloy. *Tribol Int* 1998;30:767–72. [http://dx.doi.org/10.1016/S0301-679X\(97\)00070-4](http://dx.doi.org/10.1016/S0301-679X(97)00070-4).

[11] Kim B, Mourhatch R, Aswath PB. Properties of tribofilms formed with ashless dithiophosphate and zinc dialkyl dithiophosphate under extreme pressure conditions. *Wear* 2010;268:579–91. <http://dx.doi.org/10.1016/j.wear.2009.10.004>.

[12] Zhang J, Spikes H. On the mechanism of ZDDP antiwear film formation. *Tribology Lett* 2016;63:24. <http://dx.doi.org/10.1007/s11249-016-0706-7>.

[13] Bancroft GM, Kasrai M, Fuller M, Yin Z, Fyfe K, Tan KH. Mechanisms of tribocochemical film formation: stability of tribo- and thermally-generated ZDDP films. *Tribol Lett* 1997;3:47–51.

[14] Minfray C, Martin JM, Esnouf C, Le Mogne T, Kersting R, Hagenhoff B. A multi-technique approach of tribofilm characterisation. *Thin Solid Films* 2004;447–448:272–7. [http://dx.doi.org/10.1016/S0040-6090\(03\)01064-2](http://dx.doi.org/10.1016/S0040-6090(03)01064-2).

[15] Pereira G, Lachenwitzer A, Kasrai M, Norton PR, Capehart TW, Perry TA, Cheng YT, Frazer B, Gilbert PUPA. A multi-technique characterization of ZDDP antiwear films formed on Al (Si) alloy (A383) under various conditions. *Tribol Lett* 2007;26:103–17. <http://dx.doi.org/10.1007/s11249-006-9125-5>.

[16] Nicholls MA, Norton PR, Bancroft GM, Kasrai M, Stasio GD, Wiese LM. Spatially resolved nanoscale chemical and mechanical characterization of ZDDP antiwear films on aluminum-silicon alloys under cylinder/bore wear conditions. *Tribol Lett* 2005;18:261–78. <http://dx.doi.org/10.1007/s11249-004-2752-9>.

[17] Nicholls MA, Do T, Norton PR, Kasrai M, Bancroft GM. Review of the lubrication of metallic surfaces by zinc dialkyl-dithiophosphates. *Tribol Int* 2005;38:15–39. <http://dx.doi.org/10.1016/j.triboint.2004.05.009>.

[18] Nicholls MA, Bancroft GM, Norton PR, Kasrai M, De Stasio G, Frazer BH, Wiese LM. Chemomechanical properties of antiwear films by using x-ray absorption microscopy and nano indentation techniques. *Tribol Lett* 2004;17:245–59. <http://dx.doi.org/10.1023/B:TRIL.0000032451.97552.3d>.

[19] Aktary M, McDermott MT, McAlpine GA. Morphology and nanomechanical properties of ZDDP antiwear films as a function of tribological contact time. *Tribol Lett* 2002;12:155–62.

[20] Kalin M, Oblak E, Akbari S. Evolution of the nano-scale mechanical properties of tribofilms formed from low- and high-SAPS oils and ZDDP on DLC coatings and steel. *Tribol Int* 2016;96:43–56. <http://dx.doi.org/10.1016/j.triboint.2015.12.013>.

[21] Nicholls MA, Norton PR, Bancroft GM, Kasrai M, Do T, Frazer BH, Stasio G De. Nanometer scale chemomechanical characterization of antiwear films. *Tribol Lett* 2004;17:205–16. <http://dx.doi.org/10.1023/B:TRIL.0000032447.32442.6a>.

[22] Pereira G, Munoz-Paniagua D, Lachenwitzer A, Kasrai M, Norton PR, Capehart TW, Perry TA, Cheng Y-T. A variable temperature mechanical analysis of ZDDP-derived antiwear films formed on 52100 steel. *Wear* 2007;262:461–70. <http://dx.doi.org/10.1016/j.wear.2006.06.016>.

[23] Sharma V, Doerr N, Aswath PB. Chemical-mechanical properties of tribofilms and their relationship to ionic liquid chemistry. *RSC Adv* 2016;6:22341–56. <http://dx.doi.org/10.1039/C6RA01915C>.

[24] Warren OL, Graham JF, Norton PR, Houston JE, Michalske TA. Nanomechanical properties of films derived from zinc dialkyl dithiophosphate. *Tribol Lett* 1998;4:189–98.

[25] Ye J, Kano M, Yasuda Y. Evaluation of local mechanical properties in depth in MoDTC/ZDDP and ZDDP tribocochemical reacted films by using nanoindentation. *Tribol Lett* 2002;13:41–7.

[26] Jacobs TDB, Wabiszewski GE, Goodman AJ, Carpick RW. Characterizing nanoscale scanning probes using electron microscopy: a novel fixture and a practical guide. *Rev Sci Instrum* 2016;87:013703. <http://dx.doi.org/10.1063/1.4937810>.

[27] Kim HJ, Moldovan N, Felts JR, Somnath S, Dai Z, Jacobs TDB, Carpick RW, Carlisle JA, King WP. Heated atomic force microscope cantilevers with wear-resistant ultrananocrystalline diamond tips. In: Proceedings of the 26th international conference on micro electro mechanical systems (MEMS), 2013 IEEE; 2013.

[28] Hao R, Tedstone AA, Lewis DJ, Warrens CP, West KR, Howard P, Gaemers S, Dillon SJ, O'Brien P. Property self-optimization during wear of MoS<sub>2</sub>. *ACS Appl Mater Interfaces* 2016. <http://dx.doi.org/10.1021/acsami.6b13802>.

[29] Zhang J, Spikes H. On the mechanism of ZDDP antiwear film formation. *Tribol Lett* 2016;63:1–15. <http://dx.doi.org/10.1007/s11249-016-0706-7>.

[30] Fujita H, Spikes HA. The formation of zinc dithiophosphate antiwear films. *Proc Inst Mech Eng Part J* 2004;218:265–77. <http://dx.doi.org/10.1243/1350650041762677>.

[31] Shimizu Y, Spikes HA. The tribofilm formation of ZDDP under reciprocating pure sliding conditions. *Tribol Lett* 2016;64:1–11. <http://dx.doi.org/10.1007/s11249-016-0776-6>.